

Characterization of CoRoT target fields with BEST: Identification of periodic variable stars in the IR01 field

Kabath P., Eigmüller P., Erikson A., Hedelt P., Rauer H.¹, Titz R., Wiese T.

Institut für Planetenforschung, Deutsches Zentrum für Luft- und Raumfahrt, 12489 Berlin, Germany

and

Karoff C.

Department of Physics and Astronomy, University of Aarhus, Ny Munkegade, Building 1520, DK-8000 Aarhus C, Denmark

petr.kabath@dlr.de

ABSTRACT

We report on observations of the CoRoT IR01 field with the Berlin Exoplanet Search Telescope (BEST). BEST is a small aperture telescope with a wide field of view (FOV). It is dedicated to search for variable stars within the target fields of the CoRoT space mission to aid in minimizing false-alarm rates and identify potential targets for additional science. CoRoT's observational program started in February 2007 with the "initial run" field (IR01) observed for about two months. BEST observed this field for 12 nights spread over three months in winter 2006. From the total of 30426 stars observed in the IR01 field 3769 were marked as suspected variable stars and 54 from them showed clear periodicity. From these 19 periodic stars are within the part of the CoRoT FOV covered in our data set.

Subject headings: methods: data analysis — binaries: eclipsing – stars: variables: general

¹Also: Zentrum für Astronomie und Astrophysik, Technische Universität Berlin, Germany

1. Introduction

Small ground based surveys with wide field of view (FOV) like the Berlin Exoplanet Search Telescope (BEST) (Rauer et al. 2004) can provide useful information on the identification of variable stars in the target fields of photometric space missions like CoRoT. The CoRoT mission (Baglin et al. 1998) performs observations of stellar pulsations of selected stars (asteroseismology) and photometric searches for transit events of extrasolar planets. In addition, a program on "additional science" studies is performed on dedicated objects, including variables, binaries, etc. Ground based surveys like BEST can play an important role to pre-check for stellar variability and to classify the newly detected variable stars in the stellar fields which will be later observed with CoRoT.

CoRoT has been successfully launched in December 2006 and the first scientific data are expected in early summer 2007. After the commissioning phase CoRoT began to observe the first short "initial run" field (IR01) for about two months. The following mission phases include long observational runs (150 days per each field) which are complemented with shorter runs (30 days per field) (Michel et al. 2006).

In addition to transits of extrasolar planets, transit shaped photometric signals can be caused by, for example, stellar spots, variability or eclipsing binaries. To distinguish between stellar activity and real planetary transits, prisms were mounted in front of the CoRoT detectors in the exoplanet channel in order to obtain colour information on the lightcurve (Barge et al. 2006). Due to the prism the point-spread function (PSF) covers about 80 pixels on the exoplanet detection part of the CoRoT CCDs (Boisnard & Auvergne 2006). Thus, the overlapping PSFs of stars in crowded fields may hide the signal originating from a planetary transit event. Another problem arises from the fact that transit-like lightcurves may actually be false alarms due to stellar variability. Eclipsing binary systems, especially grazing eclipses, show transit-shaped lightcurves very similar to an extrasolar planet transit. Therefore, it is of advantage to know the distribution of variable stars in the CoRoT target fields prior to the spacecraft observations. Incoming lightcurves from the spacecraft can be checked for already known variables overlapping with the selected PSF-window, or the information can be used to avoid such variables when placing the aperture windows of the satellite. For the additional science program, however, variables may be interesting targets. Information on such variable stars can be provided by a ground based survey like BEST.

BEST observes the CoRoT stellar fields in order to identify variables and to preselect interesting objects prior to CoRoT's observations. This information will be fed into the EXODAT database (Deleuil et al. 2006) which is a catalogue containing information on more than 10 millions of stars based on mainly photometric observations prepared for the CoRoT observational sequence adjusting. Here we focus on variable stars in IR01 field. The BEST

results on the stellar variability in the CoRoT LRc1 field (the first "long run" field of 150 days observing time) can be found in (Karoff et al. 2007).

The paper is arranged as follows. In the following section a short description of the BEST system is followed by a description of the observations. The third section presents the data reduction pipeline, including a description of photometric and astrometric routines used. The stellar variability characterization and the classification of the newly identified variable stars is included in the fourth section. The last section is an overview on the presented data.

2. BEST setup and observations

BEST is operated by the "Institute für Planetenforschung" of the "Deutsches Zentrum für Luft- und Raumfahrt (DLR)" and was located in Tautenburg, Germany from 2001 until 2004 (Rauer et al. 2004). It was then relocated to the Observatoire de Haute-Provence (OHP), France. BEST started to regularly observe from OHP in early 2004 with a maintenance period of three months in summer 2006 which were without observations. Since autumn 2006 the telescope is operated in remote control mode by an observer from Berlin. The primary goal of the observations is to identify new variable stars in the target field of the CoRoT mission.

BEST consists of a Schmidt-Cassegrain telescope with a 19.5 cm effective aperture and a focal ratio of $f/2.7$. The telescope is equipped with a 2048×2048 pixel CCD Apogee AP-10 with grade E chip with pixel size of $14 \times 14 \mu\text{m}$. The image scale corresponds to $5.5''$ per pixel, and the FOV is $3.1^\circ \times 3.1^\circ$. The digital resolution is 14 bit, resulting in a saturation level of 16384 ADU and a short readout time of 9 sec. The quantum efficiency of the chip reaches 40% for wavelengths within 650 – 800 nm. Observations are performed without any filter in order to achieve the maximum photonic gain. The spectral response of the CCD corresponds to a wide R -bandpass filter. Due to the large FOV BEST can detect more than 30000 stars in a typical stellar field positioned in the galactic plane.

The center of the observed IR01 field is located at $\alpha = 6^h57^m18^s$ and $\delta = -1^\circ42'00''$. The BEST FOV was oriented such that the exoplanet part of the CoRoT FOV was covered, but the very bright stars of the seismology part of the were safely avoided (see Fig. 1) - the approximate coordinates of the center of BEST FOV are $\alpha = 06^h46^m24^s$ and $\delta = -01^\circ54'00''$. We observed the IR01 field from the beginning of November, when it began to be above the horizon for more than 3 hours. The observing campaign finished in mid-December. BEST collected the data from 12 nights, spread over the whole observational period. No data were obtained at nights with bad weather conditions and around full Moon. We observed 5 nights

under very good, 5 nights under good and 2 nights under poor photometric conditions. In total we observed the field over the time span of 40.012 days.

The observing run consists of images with two different exposure times in order to cover a wide range of detectable magnitudes. A 40 second exposure was followed by 240 seconds exposures. The apparent brightness of the detected stars ranges from 8 to 18 magnitudes. A histogram of the stellar magnitudes of the 240 second exposures is shown in Figure 2. Although bright stars are detected in the frames with long exposure time, stars with magnitudes less than 10 mag can be saturated, depending on seeing and transparency, or affected by CCD non-linearities. The bright stars therefore need to be studied in the short exposures. In the following, we present only the data obtained from 300 frames with longer exposure time which corresponds to total 300 data points per lightcurve and with magnitudes > 10 mag because the faint stars overlap with the magnitude range of CoRoT (12 - 16 mag) and according to our test the CCD is working linear at these magnitudes for 240 seconds exposure time.

Each exposure sequence was followed by bias and dark frames for calibration purposes. The Apogee CCD camera is only cooled with a 2-stage thermoelectrical Peltier cooler with forced air. Cooling temperature of maximum $38^{\circ}C$ below ambient temperature can be reached but a significant dark current is detected. Variations in temperature stabilization lead to small variations in the dark current level which are monitored during the night. However, the variations are typically below 0.5% during the night. Bias level variation are at the same level. The bias frames obtained during the observations are mainly used to monitor the performance of the CCD and to clean it from any local charge levels e.g. from the saturation due to bright stars.

3. Data reduction

3.1. Basic calibrations and data pipeline

The data reduction and analysis follows (Karoff et al. 2007). In the first step a basic photometric calibration of the raw CCD data is performed, including dark current and bias subtraction as well as flatfield correction (for details see Rauer et al. (2004)). The dark and bias frames taken regularly within the observing sequence are checked for variations during the night and they are then composed into a master frames used for the calibration of the raw images, together with calibrated master flat fields. In order to perform a quick and accurate reduction of the frames which also removes the sky background, an image subtraction routine from the ISIS data reduction package (Alard & Lupton 1998) was used.

Prior to the photometric reduction an image with the best seeing from the middle of the observation run was chosen from the data set. This image was used as a template for the transformation of (x, y) coordinates of all frames into the same coordinate grid. After the coordinate transformation ISIS creates a reference frame by combination of the images with the best seeing (in the case of IR01 we used 14 images). The reference frame is then subtracted from all other images, such that each PSF of a star in each frame is convolved with the kernel of the corresponding star in the reference frame. Simultaneously the sky background is removed.

3.2. From calibrated frames to lightcurves

Photometry was performed as simple unit-weight aperture photometry on the subtracted frames and on the reference frame to obtain instrumental magnitudes. The analyzed stars have a FWHM between 1 and 3 pixels, depending on seeing. Therefore we use an aperture radius of 7 pixels, which was found to be optimal for our purposes (Karoff et al. 2007).

After applying the photometric routine, the brightest 5069 stars (magnitude limit 11.4 mag) of the BEST data set were matched with stars from the USNOA-2.0 catalogue (Monet et al. 1998). This catalog was used as reference to obtain a rough calibration of our instrumental magnitudes and to perform astrometry. We note that our variable search requires only relative magnitudes and we do not aim on an accurate absolute photometric calibration of our target stars. For the astrometric calibration, we use a cubic transformation within the MATCH routine (Valdes et al. 1995) to calculate the transformation from the (x, y) coordinates of the BEST-CCD to α and δ . A transformation of lower order did not work because of large FOV of BEST. For the matching itself we used a radius of $2 \cdot 10^{-4}$ deg. Difficulties due to multiple matches are a problem using this procedure because of the large image scale of BEST ($5.5''$ pixel $^{-1}$). However, 2945 stars could be successfully matched with the catalogue stars. The derived magnitude correction was then applied to all stars from the whole data set.

3.3. Photometric accuracy

BEST data can be affected by systematic errors due to zero-point offsets from night to night or a large scatter due to bad weather conditions. Observations of a very good night contain more than 3000 stars with rms scatter of the lightcurves less than 1%. This precision can be reached in the magnitude range 10 – 13 mag in such good nights. However

there is a clear difference between nights with good and those with bad photometric quality which is reflected by the varying number of stars having an rms below 1%. These effects can lead to a misidentification of variable stars with automatized selection routines. In order to minimize these and others effects leading to remaining systematic intensity variations in the data after application of the reduction pipeline, a cleaning algorithm (Tamuz et al. 2005) was applied four times on the whole data set. The algorithm detects systematic intensity variations affecting the whole data set (e.g. residual extinction) and therefore performs an additional photometric correction to the data. This correction is most effective for bright stars, faint stars are dominated mainly by background noise. The resulting lightcurves from the cleaning algorithm were then searched for the variable stars.

Figure 3 shows the resulting rms of the stellar lightcurves in our data versus magnitude over the whole observing campaign. About 1500 stars in the magnitude range of 10 – 12 mag have an rms level of less than 1% in the combined lightcurves, clearly showing the effect of remaining poor observing nights on the overall photometric quality. We nevertheless decided to keep all nights in the already time limited data set. The scattered very high levels of rms seen at all magnitudes are caused in part by real intrinsic variability of stars (see below), but can in part also be caused by instrumental effects, such as cosmic ray hits, stars crossing hot CCD pixels, etc., or effects by crowding and varying seeing.

The large pixel scale of BEST and the dense CoRoT field result in reduced photometric quality in very crowded areas of the field. The effects of crowding are already significantly reduced, however, by using ISIS instead of simple direct aperture photometry. Photometry is applied in reference subtracted frames with ISIS. In these frames non-variable stars cancel out and aperture photometry of the remaining variables can be performed with relatively large radius. However, in very dense areas variable stars or residuals of bright stars within the aperture of a detected star can affect the result. This leads to enhanced noise, but can also lead to multiple detections of the same variable. To avoid such false multiple variable detections, each periodic variable star was checked manually to securely identify the right object.

Variable background objects within the PSF of BEST may lead to diluted signals or may be missed as variables altogether. Identification of such background objects needs higher spatial resolution follow-up observations. Thus, the possibility that variables reported here are actually caused by background objects or unresolved stars within our PSF can not be excluded and is subject of future dedicated follow-up investigations on interesting objects.

4. Variable stars

The lightcurves resulting from our calibration pipeline and after further correction of systematic residual intensity variations by the algorithm of (Tamuz et al. 2005) are then searched for stellar variability. The motivation for our search for variable stars in the CoRoT field has been mentioned in the Introduction to this paper. Selection process, period search and classification of the identified variable stars is described here.

4.1. Criterion for variability

In order to classify the activity of the stars contained in the data set a variability index j is defined as the normalized sum of the deviations of each data point (or pair of data points with small separations in time) in the lightcurve compared to the expected noise level for the star. We changed the original definition of the Stetson’s variability index (Stetson 1996) according to Zhang et al. (2003). We used $j > 2$ as a criterion for suspected stellar variability. Figure 4 shows the index j as a function of magnitude. 3769 stars were identified as possible variables from a total number of 30426 detected stars. Figure 1 shows the spatial distribution of the suspected variables in the BEST FOV.

Only for a part of the suspected variable stars which were marked with j index a period was found. However, there will be a number of additional periodic variables, in particular long-periodic, for which periodicity can not be determined in the sparse data set. An additional fraction of the suspected variables will show real, but non-periodic variability. The remaining stars with high j index will show variability caused by instrumental effects or high noise levels remaining after photometric reduction. It is difficult to discriminate the latter from real non-periodic variables, because instrumental effects can depend on the position of a star on the CCD (e.g. hot pixels) or with time (e.g. cosmic ray hits) and thus are difficult to estimate on a statistical basis. In this paper we concentrate on periodic variable stars, because they are of most interest for CoRoT. However, the information of suspected variables with $j > 2$ will be made available to interested observers on request for further investigations.

4.2. Detected periodic variables

All lightcurves of suspected variable stars were searched for the periodicity with the method introduced by Schwarzenberg-Czerny (1996). This method fits a set of periodic orthogonal polynomials to the observational data sets and evaluates the quality of the fit

using an analysis of variance statistics. All suspected variables with fit quality better than 0.9 were examined visually. Most rejected of suspected variable stars show periods close to one day or multiples of one day and show no clear evidence of at least two maxima or minima in the lightcurve. This rejected variability is very likely caused by changes of the background level, temperature, airmass or by instrumental effects.

In total, 54 stars were classified as periodic variable stars after the visual check. Periods were searched between 0.1 day up to 10 days. The details about the stars are listed in Table 1. A distribution of these newly detected periodic variable stars over the BEST FOV and also within the CoRoT IR01 field covered can be seen in Figure 1. The number of variable stars detected in the CoRoT FOV covered by our observations is 19 and they are marked with a star in Table 1. The finding charts will be provided upon a request.

We compared the periodic variable stars identified with the GCVS catalogue via SIMBAD coordinates query. Two BEST stars (ID 2109 and 2390) were already present in GCVS: *V453 Mon* and *V515 Mon*. In total, 52 of our variable stars are new discoveries.

The completeness of our data set is restricted. We have been able to detect only short periodic variable stars due to bad weather conditions in mid November and in general due to the short observing run. The IR01 field was observable from 3 (at the beginning of November) to a maximum of 6 (mid December) hours per night only. Therefore the periods of detected variable stars found are usually below 1 day. The following stars showed periods longer than one day: ID 1101, 1180, 1194, 1239, 1549, 1865, 1993, 2440, 2632, 2633, 2651, 2661, 3175 and 3203. Star 1194 is located near to a bright star for which a reasonable match is the star HD295427, however it is not possible to decide which star from both of them is the variable star. Star 2349 shows a "corrupted" lightcurve which may be due to nearby star 2354.

The classification of the periodic variable stars is based on the GCVS (see Sterken & Jaschek, 1996). As only a limited amount of information is available at lightcurves contained in our data set – i.e. we do not have any spectral or color information, we have not been able to make a full classification into all the classification classes given by the GCVS. The classes we have used are: CEP, DSCT, ELL, EA, EB and EW.

The main separation in the classification is between pulsating periodic variable stars, eclipsing binaries and rotating stars. This classification is relatively straight forward to make. The pulsating variable stars have been separated in to CEP and DSCT based on the period. Stars with period below 0.3 days were classified as DSCT and stars with periods longer than 0.3 days were classified as CEP stars what is based on the earlier usage of the CEP class without subdivisions. Thus CEP refers here to all kind of pulsating periodic stars

with periods longer than 0.3 days, e.g. BCEP, CEP, DCEP, RR as the information does not allow the classification into the subclasses. For the DSCT with periods below 0.3 days the classification should be fairly unique. The classification for the rotating stars ELL is based on the unequal minima/maxima of the lightcurves.

The eclipsing binaries have been separated into EA, EB and EW classes based on the criteria given by Sterken & Jaschek (1996) – i.e EA class shows constant lightcurves between eclipses, EB class varies continuously between eclipses and stars belonging to the EW class have equal depth and periods shorter than 1 day.

The stars 1194, 1898 and 2633 show clear variability, but no clear period. We expect that the stars are either multiperiodic pulsating stars (e.g. BCEP, SPB, γ Dor stars) or rotating spotted stars. However more data with better duty cycle is needed to make a precise classification. Such data will be provided with CoRoT. These three stars are marked in the Table 1 with ?.

5. Summary

The BEST telescope was used to search for short-period variables within the CoRoT exoplanet channel FOV of the IR01 field. In total 54 periodic variable stars were detected and 52 of them are new discoveries. From these stars, 19 are within the part of the CoRoT field covered in our observations. All detected variables are short period (mainly $P < 1$ day), because of the limited data set. Nevertheless, the variables found will give some additional information when analysing CoRoT PSFs near these variables and will help avoiding false-alarms in case of potential transit candidate signals nearby.

The authors gratefully acknowledge the support and assistance of the staff at Observatoire de Haute-Provence. We are also most grateful to an anonymous referee for his helpful comments and useful advice.

We would like to greatly appreciate the help of Sabrina Kirste who contributed to preparing of the manuscript. C. K. acknowledges support from Danish AsteroSeismology Centre and Instrument Center for Danish Astrophysics. The support to DLR staff in observational tasks given by Berlin local amateur astronomers Susanne Hoffman, Irene Berndt, Martin Dentel and Karsten Markus is also greatly acknowledged. We made use of SIMBAD and GCVS catalogues.

REFERENCES

- Alard, C. & Lupton, R. H. 1998, *ApJ*, 503, 325
- Baglin, A., Auvergne, M., Barge, P., Buey, J.-T., Catala, C., Michel, E., Weiss, W., & CoRoT Team 2002, ESA SP-485: Stellar Structure and Habitable Planet Finding, 17
- Barge, P., Leger, A., Ollivier, M., Rouan, D., Schneider, J., and the Exoplanet CoRoT Team 2006, ESA SP-1306: The CoRoT Mission, 83
- Boisnard, L., Auvergne, M. 2006, ESA SP-1306: The CoRoT Mission, 19
- Deleuil, M., Moutou, C., Deeg, H., J., Meunier, J., C., Surace, C., Guterman, P., Almenara, J. M., Alonso, R., Barge, P., Bouchy, F., Erikson, A., Leger, A., Loeillet, B., Ollivier, M., Pont, F., Rauer, H., Rouan, D., and Queloz, D. 2006, ESA SP-1306: The CoRoT Mission, 341
- Frandsen, S., Jones, A., Kjeldsen, H., Viskum, M., Hjorth, J., Andersen, N. H., & Thomsen, B. 1995, *A&A*, 301, 123
- Karoff, C., Rauer, H., Erikson, A., Voss, H., Deleuil, M., Moutou, C., Meunier, J., C., Deeg, H. 2007, accepted to *AJ*
- Lomb, N. R. 1976, *Ap&SS*, 39, 447
- Michel, E., Deleuil, M., and Baglin, A. 2006, ESA SP-1306: The CoRoT Mission, 473
- Monet, D., et. al. 1998, The PMM USNO-A2.0 Catalogue. (1998)
- Rauer, H., Eislöffel, J., Erikson, A., Guenther, E., Hatzes, A. P., Michaelis, H., Voss, H. 2004, *PASP*, 116, 38
- Schwarzenberg-Czerny, A. 1996, *ApJ*, 460, 107
- Sterken, C., Jaschek, C., 1996, *Light curves of variable stars*, Cambridge University press
- Stetson, P. B. 1996, *PASP*, 108, 851
- Tamuz, O., Mazeh, T. and Zucker, S. 2005, *MNRAS*, 356, 1466
- Valdes, F. G., Campusano, L. E., Velasquez, J. D., & Stetson, P. B. 1995, *PASP*, 107, 1119
- Zhang, X., Deng, L., Xin, Y., & Zhou, X. 2003, *Chinese Journal of Astronomy and Astrophysics*, 3, 151

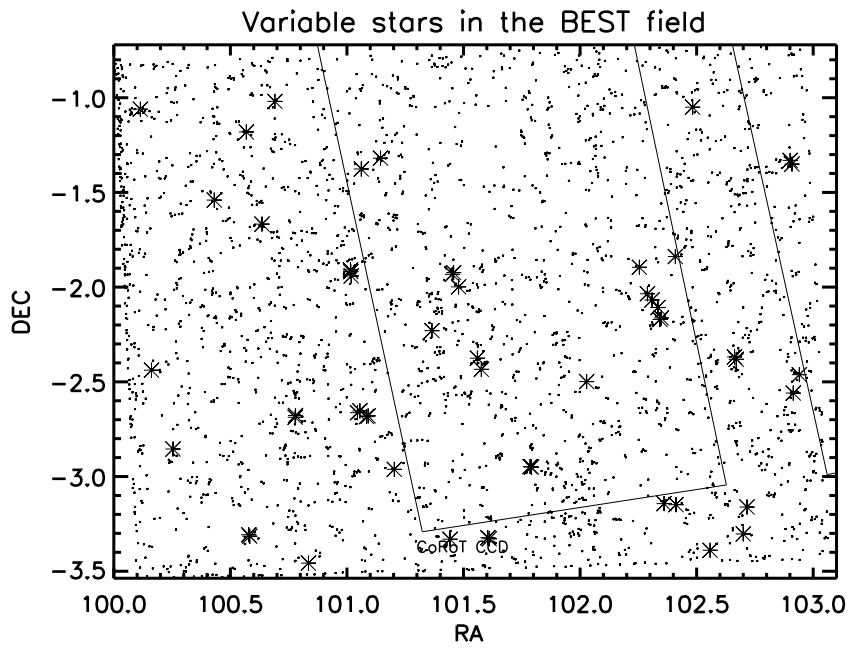


Fig. 1.— The CoRoT IR01 field is indicated in the BEST field. The distribution of the variable stars found in the BEST FOV is shown. Dots show stars with $j > 2$ and stars are periodic variables selected visually from the stars having $j > 2$.

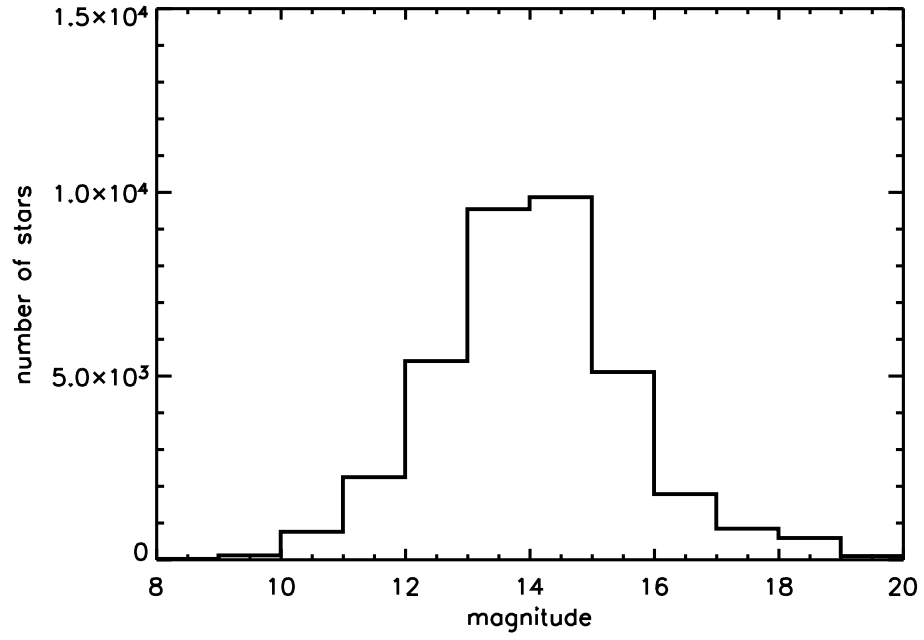


Fig. 2.— Histogram of magnitudes of the detected stars in the BEST FOV.

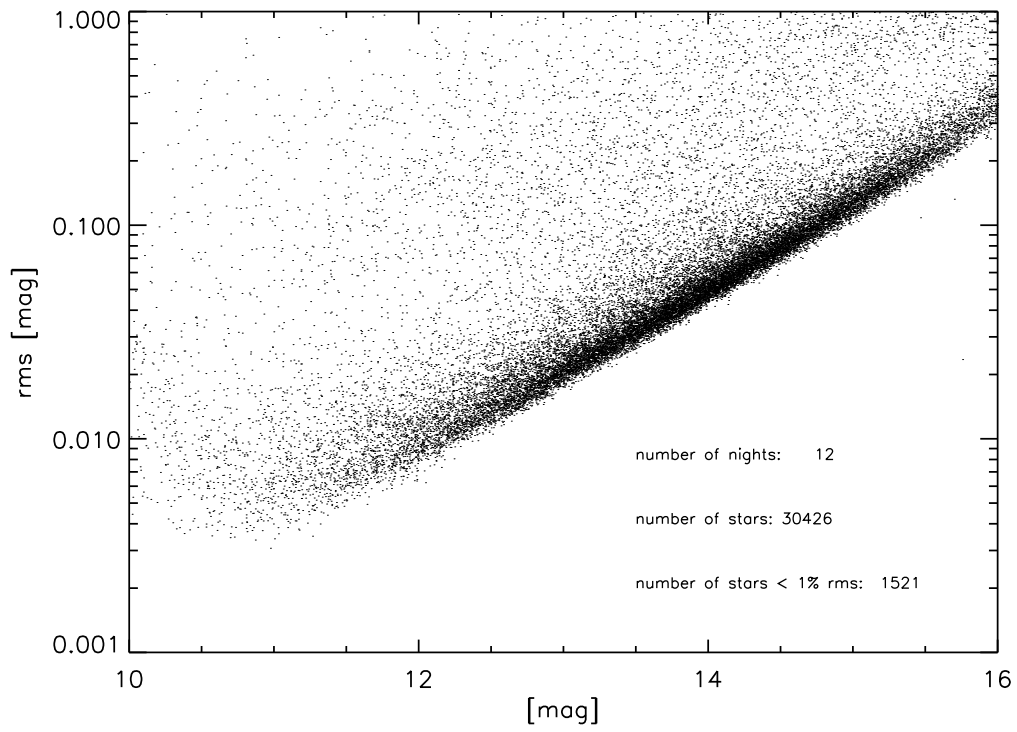


Fig. 3.— The rms noise level of stellar lightcurves for the whole data set over magnitude over the observing campaign.

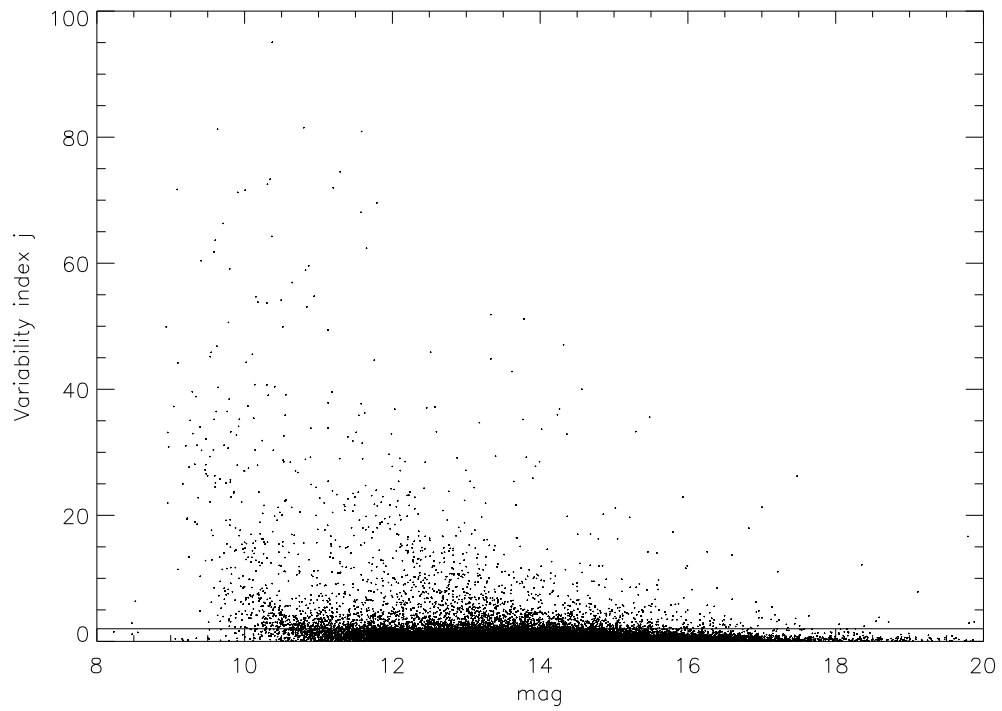
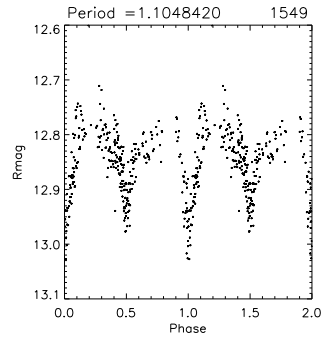
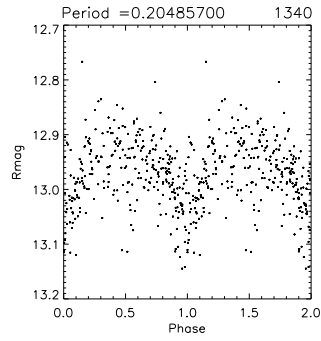
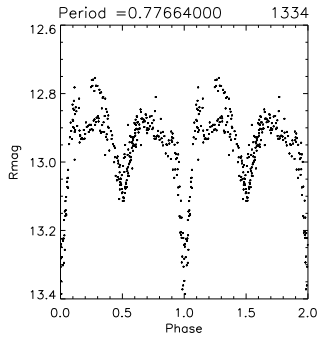
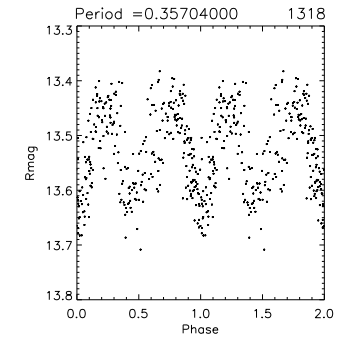
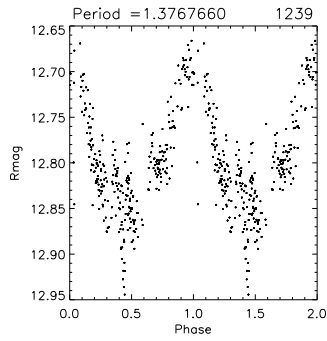
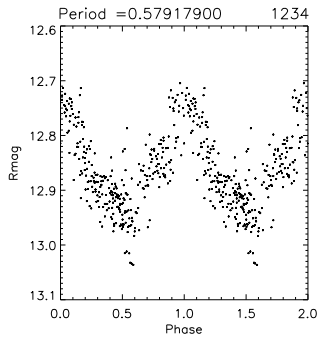
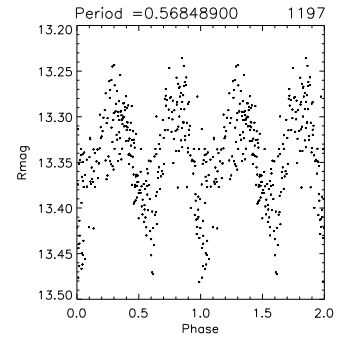
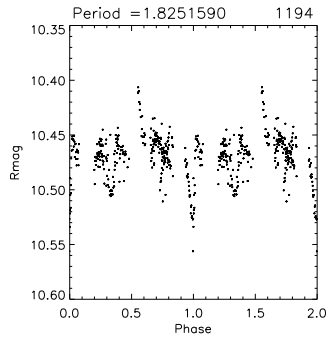
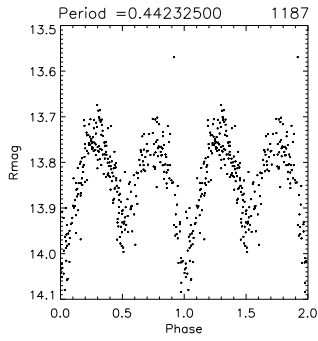
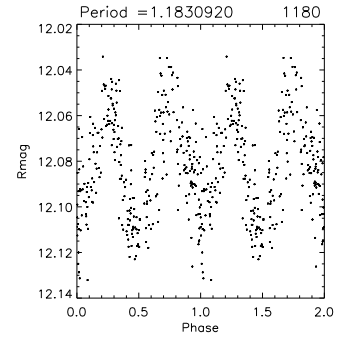
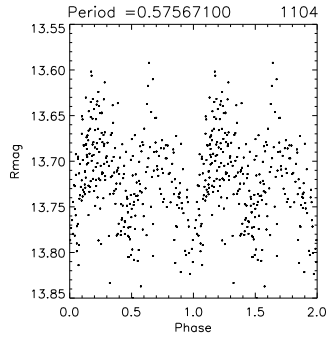
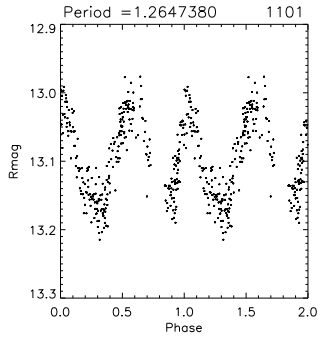
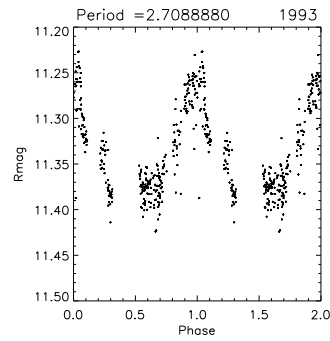
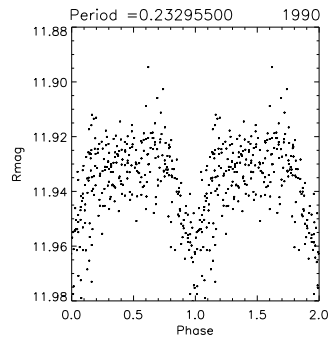
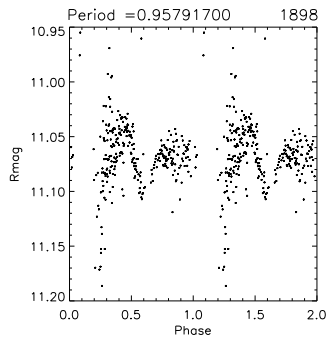
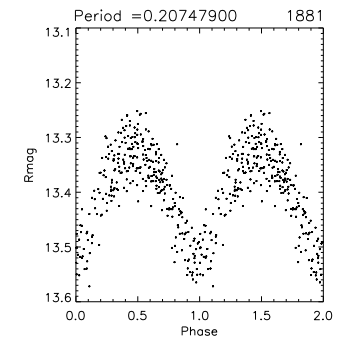
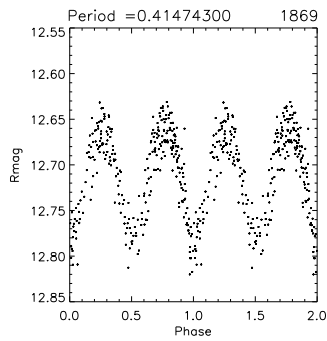
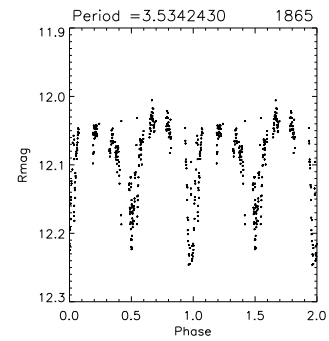
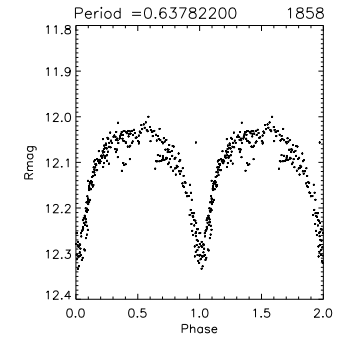
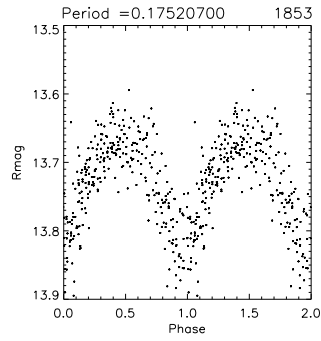
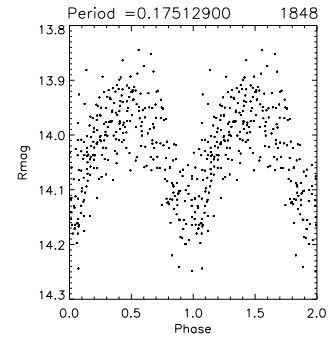
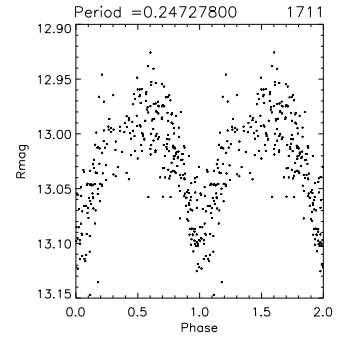
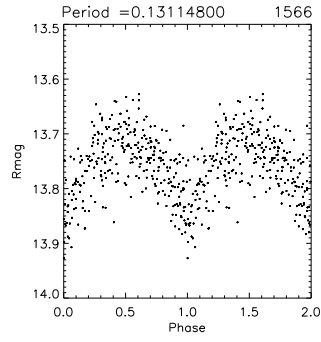
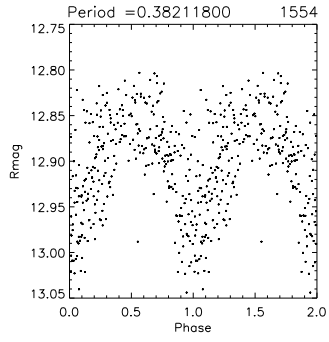
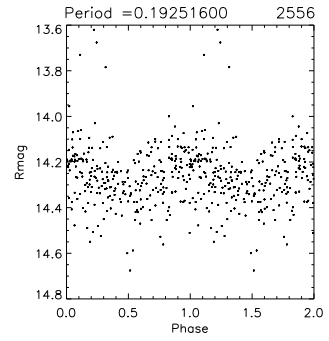
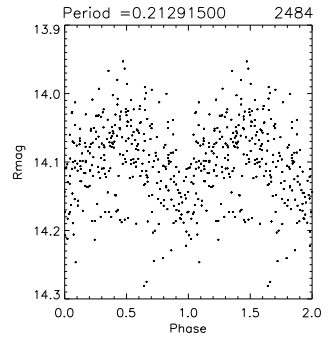
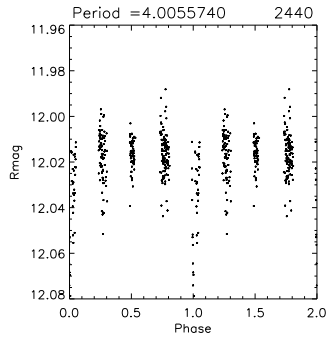
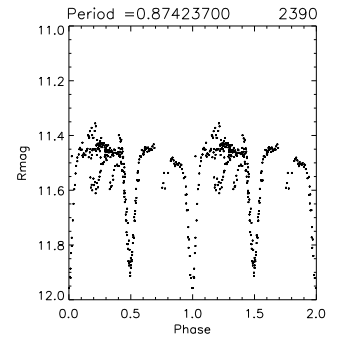
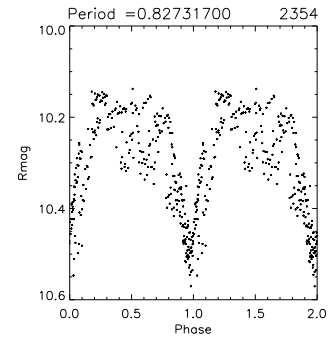
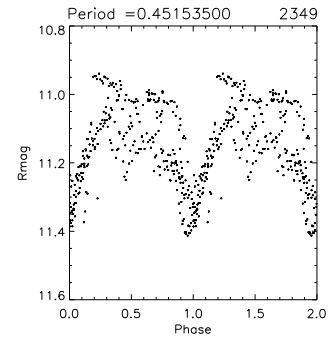
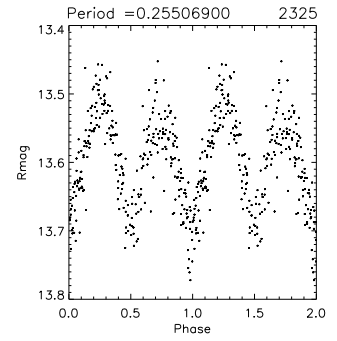
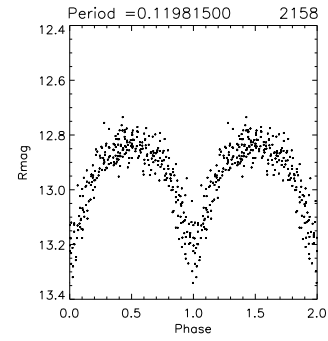
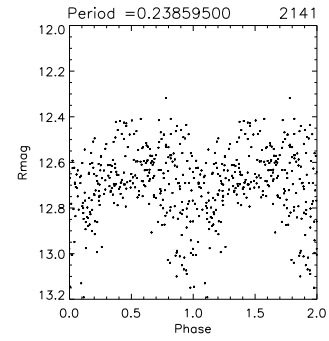
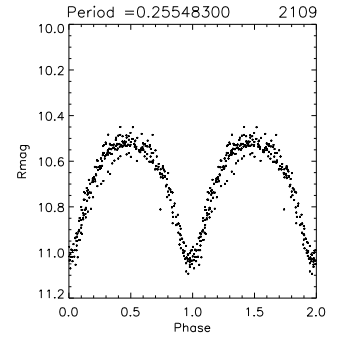
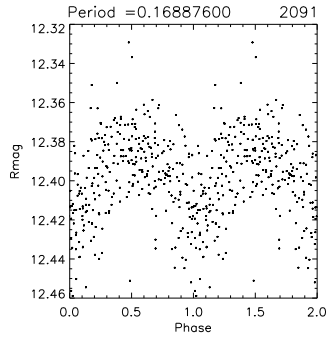
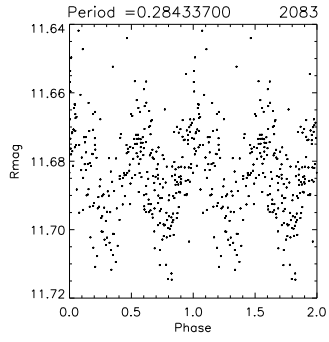
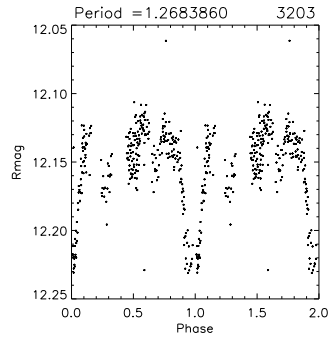
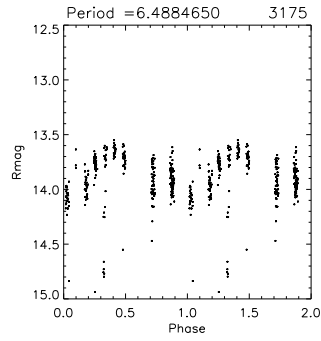
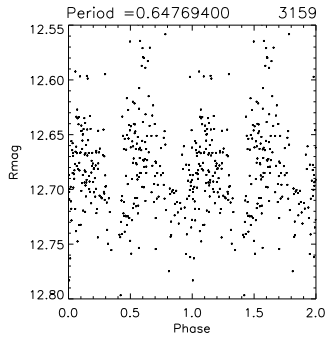
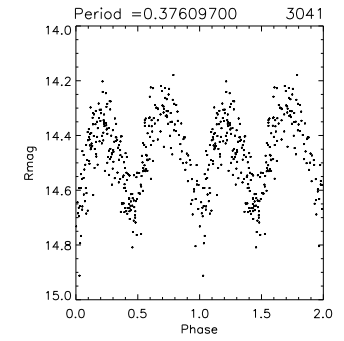
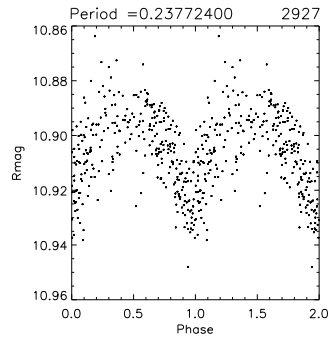
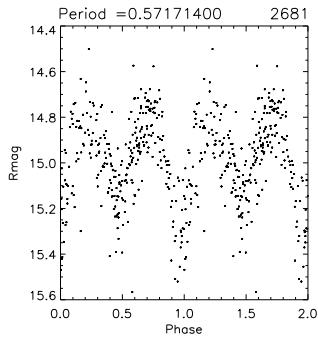
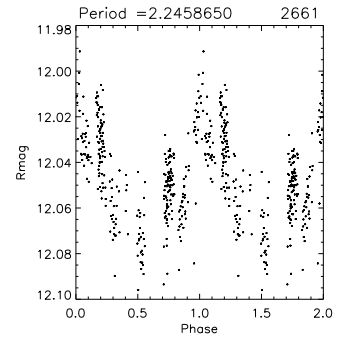
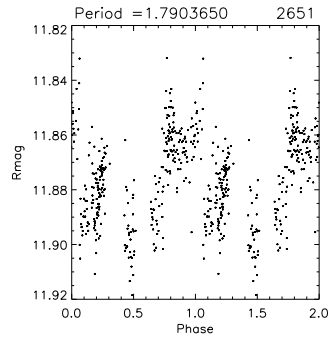
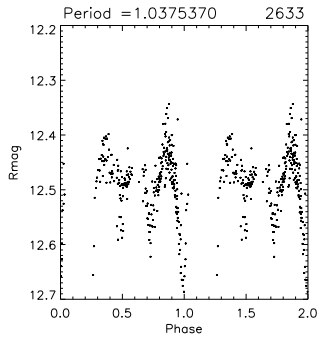
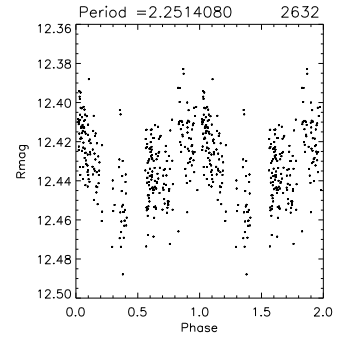
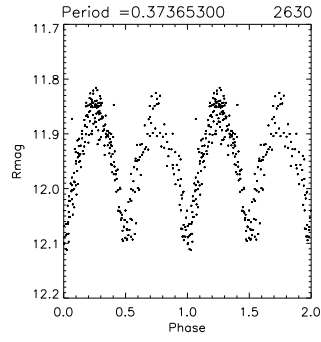
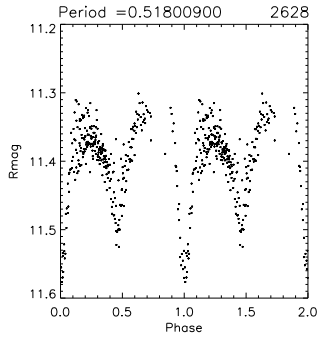


Fig. 4.— Variability index j of the sample plotted over magnitudes of the stars. The line marks the limit of $j = 2$ used to identify suspected variable stars.









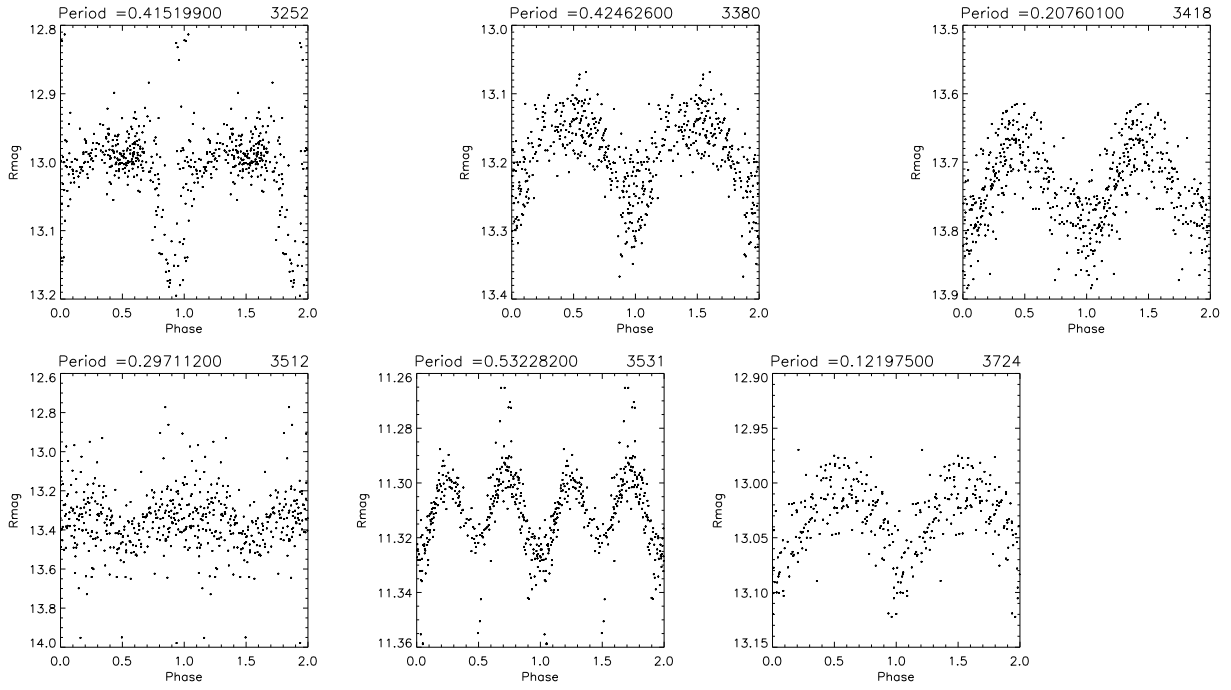


Fig. 5.— Phased lightcurves of periodic variables. The BEST-ID is shown in the upper right corner of each graph.

Table 1. Periodic variable stars detected. Magnitudes are based on calibration against USNO catalogue only. IDs marked with a star are within CoRoT field of view.

BEST ID	α (J2000)	δ (J2000)	Period(days)	Mean mag	Amplitude(mag)	Type
1101	$06^h 43^m 20^s$	$-3^\circ 27' 25.5''$	1.265	13.10	0.20	ELL
1104	$06^h 50^m 14^s$	$-3^\circ 23' 21.0''$	0.576	13.72	0.19	CEP
1180	$06^h 50^m 48^s$	$-3^\circ 18' 11.3''$	1.183	12.08	0.07	ELL
1187	$06^h 46^m 26^s$	$-3^\circ 19' 42.7''$	0.442	13.82	0.40	EB
1194	$06^h 45^m 46^s$	$-3^\circ 19' 51.7''$	1.825	10.47	0.10	?
1197	$06^h 46^m 25^s$	$-3^\circ 19' 22.2''$	0.569	13.34	0.21	CEP
1234	$06^h 42^m 20^s$	$-3^\circ 18' 54.3''$	0.579	12.88	0.25	CEP
1239	$06^h 42^m 19^s$	$-3^\circ 18' 25.9''$	1.377	12.81	0.27	CEP
1318	$06^h 50^m 52^s$	$-3^\circ 09' 39.9''$	0.357	13.53	0.29	EW
1334	$06^h 49^m 39^s$	$-3^\circ 08' 54.6''$	0.777	12.94	0.60	EB
1340	$06^h 49^m 26^s$	$-3^\circ 08' 34.8''$	0.205	12.98	0.28	EW
1549*	$06^h 47^m 10^s$	$-2^\circ 57' 0.7''$	1.105	12.85	0.30	EB
1554*	$06^h 47^m 09^s$	$-2^\circ 56' 52.0''$	0.382	12.90	0.23	EW
1566	$06^h 44^m 49^s$	$-2^\circ 57' 43.4''$	0.131	13.75	0.26	EW
1711	$06^h 41^m 01^s$	$-2^\circ 51' 17.2''$	0.247	13.02	0.17	EW
1848	$06^h 44^m 20^s$	$-2^\circ 41' 0.2''$	0.175	14.02	0.30	EW
1853	$06^h 44^m 22^s$	$-2^\circ 40' 47.7''$	0.175	13.72	0.20	EW
1858	$06^h 43^m 07^s$	$-2^\circ 41' 13.2''$	0.638	12.10	0.30	EA

Table 1—Continued

BEST ID	α (J2000)	δ (J2000)	Period(days)	Mean mag	Amplitude(mag)	Type
1865	06 ^h 43 ^m 07 ^s	-2° 40' 40.0"	3.534	12.08	0.21	EB
1869	06 ^h 44 ^m 10 ^s	-2° 39' 45.6"	0.415	12.69	0.18	EW
1881	06 ^h 44 ^m 13 ^s	-2° 39' 11.4"	0.208	13.38	0.32	EW
1898	06 ^h 51 ^m 39 ^s	-2° 33' 33.6"	0.958	11.07	0.07	?
1990*	06 ^h 48 ^m 07 ^s	-2° 29' 55.0"	0.233	11.94	0.06	EA
1993*	06 ^h 51 ^m 46 ^s	-2° 27' 43.9"	2.709	11.35	0.15	ELL
2083*	06 ^h 46 ^m 18 ^s	-2° 26' 2.4"	0.284	11.68	0.04	DSCT
2091*	06 ^h 50 ^m 41 ^s	-2° 22' 51.8"	0.169	12.40	0.07	DSCT
2109	06 ^h 50 ^m 39 ^s	-2° 22' 6.7"	0.256	10.66	0.60	EW
2141	06 ^h 40 ^m 39 ^s	-2° 26' 18.9"	0.239	12.68	0.60	DSCT
2158	06 ^h 46 ^m 14 ^s	-2° 22' 30.8"	0.120	12.91	0.50	EW
2325*	06 ^h 45 ^m 27 ^s	-2° 13' 47.6"	0.255	13.59	0.26	EW
2349*	06 ^h 49 ^m 22 ^s	-2° 10' 15.6"	0.452	11.16	0.40	EB
2354*	06 ^h 49 ^m 24 ^s	-2° 09' 45.8"	0.827	10.31	0.40	EB
2390*	06 ^h 49 ^m 21 ^s	-2° 06' 48.5"	0.874	11.60	0.50	EB
2440	06 ^h 49 ^m 14 ^s	-2° 04' 04.4"	4.006	12.02	0.08	CEP
2484*	06 ^h 49 ^m 09 ^s	-2° 02' 06.4"	0.213	14.10	0.22	DSCT
2556*	06 ^h 45 ^m 55 ^s	-1° 59' 54.4"	0.193	14.26	0.30	DSCT
2628*	06 ^h 45 ^m 49 ^s	-1° 55' 57.0"	0.518	11.39	0.26	EB
2630*	06 ^h 49 ^m 01 ^s	-1° 53' 42.8"	0.374	11.93	0.28	EW
2632	06 ^h 44 ^m 04 ^s	-1° 56' 27.6"	2.251	12.43	0.05	CEP
2633	06 ^h 45 ^m 50 ^s	-1° 55' 24.2"	1.038	12.49	0.30?	?
2651	06 ^h 44 ^m 04 ^s	-1° 55' 05.0"	1.790	11.88	0.07	CEP
2661	06 ^h 44 ^m 04 ^s	-1° 54' 33.5"	2.246	12.05	0.09	CEP
2681*	06 ^h 49 ^m 38 ^s	-1° 50' 18.9"	0.572	14.98	0.80	EW
2927	06 ^h 42 ^m 33 ^s	-1° 40' 02.1"	0.238	10.91	0.05	EW
3041	06 ^h 41 ^m 43 ^s	-1° 32' 25.8"	0.376	14.47	0.60	EW
3159	06 ^h 51 ^m 38 ^s	-1° 21' 01.4"	0.648	12.69	0.14	CEP
3175*	06 ^h 51 ^m 36 ^s	-1° 19' 51.1"	6.489	13.89	0.65	CEP
3203*	06 ^h 44 ^m 15 ^s	-1° 22' 34.7"	1.268	12.15	0.15	EA
3252*	06 ^h 44 ^m 35 ^s	-1° 19' 08.7"	0.415	13.00	0.24	EA

Table 1—Continued

BEST ID	α (J2000)	δ (J2000)	Period(days)	Mean mag	Amplitude(mag)	Type
3380	$06^h 42^m 16^s$	$-1^\circ 10' 50.9''$	0.425	13.18	0.25	EW
3418	$06^h 49^m 56^s$	$-1^\circ 02' 59.3''$	0.208	13.74	0.25	EW
3512	$06^h 40^m 27^s$	$-1^\circ 03' 38.3''$	0.297	13.35	0.50	DSCT
3531	$06^h 42^m 46^s$	$-1^\circ 01' 09.7''$	0.532	11.31	0.04	EB
3724*	$06^h 45^m 39^s$	$-0^\circ 47' 33.8''$	0.122	13.03	0.03	EW